
PERGAMON

Journal of Quantitative Spectroscopy & Radiative Transfer 73 (2002) 571–582

Journal of Quantitative Spectroscopy & Radiative Transfer

www.elsevier.com/locate/jqsrt

Non-Fourier heat conduction with radiation in an absorbing, emitting, and isotropically scattering medium

Hsin-Sen Chu[a,*], Senpuu Lin[b], Chia-Hui Lin[a]

[a] *Department of Mechanical Engineering, National Chiao Tung University, 1001 Ta Hsueh Road, Hsinchu 30010, Taiwan, ROC*

[b] *Department of Mechanical Engineering, National Lien Ho Institute of Technology, Miaoli 360, Taiwan, ROC*

Received 23 April 2001; received in revised form 5 June 2001; accepted 5 June 2001

Abstract

This article numerically analyses the combined conductive and radiative heat transfer in an absorbing, emitting, and isotropically scattering medium. The non-Fourier heat conduction equation, which includes the time lag between heat flux and the temperature gradient, is used to model the conductive heat transfer in the medium. It predicts that a temperature disturbance will propagate as a wave at finite speed. The radiative heat transfer is solved using the P_3 approximation method. In addition, the MacCormack's explicit predictor–corrector scheme is used to solve the non-Fourier problem. The effects of radiation including single scattering albedo, conduction-to-radiation parameter, and optical thickness of the medium on the transient and steady state temperature distributions are investigated in detail. Analysis results indicate that the internal radiation in the medium significantly influences the wave nature. The thermal wave nature in the combined non-Fourier heat conduction with radiation is more obvious for large values of conduction-to-radiation parameter, small values of optical thickness and higher scattering medium. The results from non-Fourier-effect equation are also compared to those obtained from the Fourier equation. Non-Fourier effect becomes insignificant as either time increases or the effect of radiation increases.

Keywords: Non-Fourier conduction; Transient coupled conductive-radiative heat transfer; Absorbing; Emitting; Isotropically scattering medium

1. Introduction

The analysis of heat transfer by simultaneous conduction and radiation in an absorbing, emitting, and scattering medium has been of considerable practical importance in many engineering

* Corresponding author. Tel.: +886-3-571-2121 ext. 55115; fax: +886-3-572-7930.
E-mail addresses: hschu@cc.nctu.edu.tw (H.-S. Chu), spuulin@mail.nlhu.edu.tw (S. Lin).

0022-4073/02/$ - see front matter
PII: S0022-4073(01)00180-7

applications involving fire protection, manufacturing of glass, fibrous and foam insulation, crystal growth, laser processing of semiconductors, etc. It has thus been the subject of numerous investigations [1–14]. Most of the previous studies dealt with the conduction heat transfer using the classical heat conduction theory, Fourier's law, which postulates that a local change in temperature causes instantaneous temperature perturbations at all regions in the medium. In other words, heat propagates at infinite speed. However, in situations dealing with cryogenic temperature, extremely short times, high-rate change of temperature or heat flux, the validity of infinite heat-propagation speed is restricted. Several investigations have indicated that the finite heat-propagation speed becomes dominant [15–23]. Özisik and Tzou [15] gave an excellent review on the research emphasizing engineering applications of the thermal wave theory. The finite speed of heat propagation may have to be considered in modeling the conduction heat transfer with radiation in an absorbing and emitting medium. Due to the complexity of radiative heat transfer phenomenon and the numerical instability of hyperbolic system, the combined effect of non-Fourier heat conduction and radiation is rarely investigated. Glass et al. [24] examined combined conduction and radiation using non-Fourier law with hyperbolic heat conduction model in an absorbing and emitting medium for the cases of a constant and a pulsed heat flux boundary. For optically thin, the wave nature gave rise to a thermal front propagating from the back surface which resulted from the heating of the back surface by radiation through the medium. While, the scattering effect was not taken into account in their investigation.

It is well known that the scattering of thermal radiation by real particles or impurities in a medium can play a significant role in the overall heat transfer [4–6,9,10,12,14]. The present work is focused on the transient interaction of non-Fourier heat conduction and radiation in an absorbing, emitting, and gray medium with the effect of isotropic scattering. The effects of radiation including single scattering albedo, conduction-to-radiation parameter, and optical thickness of the medium on the transient and steady state temperature distributions are examined in detail. The results from non-Fourier heat conduction equation are also compared to those obtained from the corresponding Fourier equation.

2. Physical model and theoretical analysis

Consider an absorbing, emitting and isotropically scattering planar medium that is initially at a uniform temperature T_0, confined to the domain $0 \leqslant x \leqslant L$ as illustrated in Fig. 1. For times greater than zero, the two boundary surfaces are kept at a specified temperature of T_L and T_R, respectively. To consider the finite speed of heat propagation for non-Fourier heat flux q^c, a damped-wave model has been proposed by Joseph and Preziosi [25] that uses a variety of reasonings and derivations. Cattaneo [26] and Vernotte [27] independently suggested a modified heat conduction model in the form of

$$q^c(x, t + \Omega) = -k\nabla T(x, t), \tag{1}$$

where Ω is the mean relaxation time of the conductive heat carriers, k the thermal conductivity, x the position vector, and t the physical time. Eq. (1) implies that the temperature gradient established at time t, due to insufficient response time, results in a heat flux vector at a later time $t + \Omega$. This means that the heat wave model of non-Fourier heat conduction allows a time

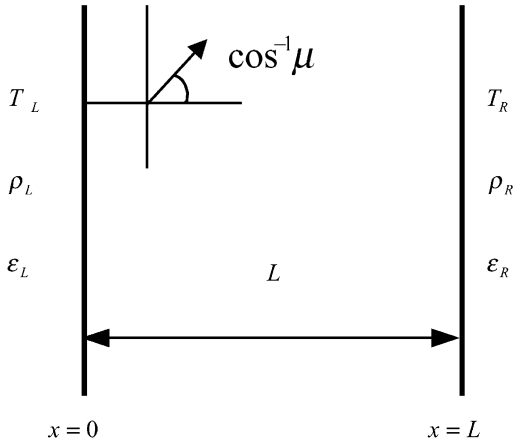

Fig. 1. Physical model and coordinate system.

lag between the heat flux and the temperature gradient. Based on the ideas from the collision theory of molecules, $\Omega = \alpha/C^2$, where C is the thermal wave velocity in the medium and α the thermal diffusivity of the medium. Obviously, as $C \to \infty$ we have $\Omega \to 0$, and the Fourier heat flux equation is obtained.

After applying Taylor's series expansion to heat flux q^{c} in Eq. (1) with respect to Ω, the linearized non-Fourier constitutive conductive equation is written as

$$q^{\mathrm{c}}(x,t) + \Omega \frac{\partial q^{\mathrm{c}}(x,t)}{\partial t} = -k\nabla T(x,t). \tag{2}$$

The energy equation for combined conduction and radiation in a participating medium with constant properties is given as

$$\rho_d c_p \frac{\partial T(x,t)}{\partial t} = -\nabla[q^{\mathrm{c}}(x,t) + q^{\mathrm{r}}(x,t)], \tag{3}$$

where $q^{\mathrm{r}}(x,t)$ is the net radiation heat flux, ρ_d the density and c_p the constant-pressure specific heat of the medium.

The intensity of radiation I, depends only on x and μ, satisfies the radiative transfer equation

$$\frac{\mu}{\beta}\frac{\partial I(x,\mu)}{\partial x} = -I(x,\mu) + (1-\omega)I_b(x) + \frac{\omega}{2}\int_{-1}^{1} I(x,\mu')p(\mu,\mu')\,\mathrm{d}\mu', \tag{4}$$

where $\mu = \cos\theta$, β is the extinction coefficient, ω is the single scattering albedo, and $p(\mu,\mu')$ is the phase function.

The boundary conditions for the intensities of diffuse boundaries are

$$I^{+}(0) = \varepsilon_{\mathrm{L}} I_b(T_{\mathrm{L}}) + 2\rho_{\mathrm{L}} \int_0^1 I^{-}(0,\mu')\mu'\,\mathrm{d}\mu', \quad 1 \geqslant \mu > 0, \tag{5a}$$

$$I^{-}(L) = \varepsilon_{\mathrm{R}} I_b(T_{\mathrm{R}}) + 2\rho_{\mathrm{R}} \int_0^1 I^{+}(L,\mu')\mu'\,\mathrm{d}\mu', \quad -1 \leqslant \mu < 0, \tag{5b}$$

where ε and ρ are the emissivity and reflectivity, respectively. Assuming the boundaries are under thermal equilibrium and opaque, that is $\alpha_j = \varepsilon_j$ and $\rho_j + \alpha_j = 1$, where $j = \mathrm{L}, \mathrm{R}$ represent the left and right boundary, respectively.

Since Eq. (4) is an integral-differential equation, a closed-form solution is not available. Ratzel and Howell [7] concluded that for one-dimensional planar problems, the P_3 approximation method yields results in close agreement with 'exact' solutions. By using P_3 approximation method, the intensity of radiation $I(x, \mu')$ and the phase function $p(\mu, \mu')$ can be assumed to represent as a series of Legendre polynomials. After rearranging, a set of differential equations is obtained

$$\frac{\mathrm{d}\psi_1(\tau)}{\mathrm{d}\tau} + (1-\omega)\psi_0(\tau) = 4\pi(1-\omega)\sigma T^4(x), \tag{6a}$$

$$2\frac{\mathrm{d}\psi_2(\tau)}{\mathrm{d}\tau} + \frac{\mathrm{d}\psi_0(\tau)}{\mathrm{d}\tau} + 3\psi_1(\tau) = 0, \tag{6b}$$

$$3\frac{\mathrm{d}\psi_3(\tau)}{\mathrm{d}\tau} + 2\frac{\mathrm{d}\psi_1(\tau)}{\mathrm{d}\tau} + 5\psi_2(\tau) = 0, \tag{6c}$$

$$3\frac{\mathrm{d}\psi_2(\tau)}{\mathrm{d}\tau} + 7\psi_3(\tau) = 0, \tag{6d}$$

where σ is the Stefan–Boltzmann constant, $\tau = \beta x$ is the optical variable, and ψ_0, ψ_1, ψ_2 and ψ_3 are the incident radiation, the radiative heat flux, the second, and third moments of the incident radiation, respectively.

Applying the Marshak's boundary conditions yields the following set of equations for the boundaries:

$$(1-\rho_\mathrm{L})\psi_0(0) + 2(1+\rho_\mathrm{L})\psi_1(0) + \frac{5}{4}(1-\rho_\mathrm{L})\psi_2(0) = 4\varepsilon_\mathrm{L}\sigma T_\mathrm{L}^4, \tag{7a}$$

$$(1-\rho_\mathrm{L})\psi_0(0) + \frac{12}{5}(1+\rho_\mathrm{L})\psi_1(0) + \frac{5}{2}(1-\rho_\mathrm{L})\psi_2(0) + \frac{8}{5}(1+\rho_\mathrm{L})\psi_3(0) = 4\varepsilon_\mathrm{L}\sigma T_\mathrm{L}^4, \tag{7b}$$

$$(1-\rho_\mathrm{R})\psi_0(\tau_0) - 2(1+\rho_\mathrm{R})\psi_1(\tau_0) + \frac{5}{4}(1-\rho_\mathrm{R})\psi_2(\tau_0) = 4\varepsilon_\mathrm{R}\sigma T_\mathrm{R}^4, \tag{7c}$$

$$(1-\rho_\mathrm{R})\psi_0(\tau_0) - \frac{12}{5}(1+\rho_\mathrm{R})\psi_1(\tau_0) + \frac{5}{2}(1-\rho_\mathrm{R})\psi_2(\tau_0) - \frac{8}{5}(1+\rho_\mathrm{R})\psi_3(\tau_0) = 4\varepsilon_\mathrm{R}\sigma T_\mathrm{R}^4. \tag{7d}$$

For convenience in the subsequent analysis, the dimensionless schemes are defined as follows:

$$\theta = \frac{T - T_0}{T_0}, \qquad \xi = \frac{Ct}{L}, \qquad \eta = \frac{x}{L}, \qquad Q^\mathrm{c} = \frac{q^\mathrm{c}}{\sigma T_0^4}, \qquad Q^\mathrm{r} = \frac{q^\mathrm{r}}{\sigma T_0^4},$$

$$N=\frac{\rho_d c_p T_0 C}{\sigma T_0^4},\qquad M=\frac{LC}{\alpha},\qquad \mathrm{d}\tau=\beta\,\mathrm{d}x,\qquad \tau_0=\beta L,$$

$$\tilde{\psi}_0=\frac{\psi_0}{\sigma T_0^4},\qquad \tilde{\psi}_1=\frac{\psi_1}{\sigma T_0^4},\qquad \tilde{\psi}_2=\frac{\psi_2}{\sigma T_0^4},\qquad \tilde{\psi}_3=\frac{\psi_3}{\sigma T_0^4}. \tag{8}$$

The energy equation (3) and non-Fourier heat conduction equation (2) are expressed in terms of the above dimensionless variables as

$$\frac{\partial\theta(\eta,\xi)}{\partial\xi}+\frac{1}{N}\frac{\partial Q^{\mathrm{c}}(\eta,\xi)}{\partial\eta}+\frac{1}{N}\frac{\partial Q^{\mathrm{r}}(\eta,\xi)}{\partial\eta}=0, \tag{9}$$

$$\frac{\partial Q^{\mathrm{c}}(\eta,\xi)}{\partial\xi}+N\frac{\partial\theta(\eta,\xi)}{\partial\eta}+MQ^{\mathrm{c}}(\eta,\xi)=0. \tag{10}$$

The initial condition is expressed as

$$\xi=0,\qquad \theta=\theta_0,\qquad Q^{\mathrm{c}}=0,\qquad Q^{\mathrm{r}}=0, \tag{11}$$

and the boundary conditions are written as

$$\theta=\theta_{\mathrm{L}}\quad\text{at }\eta=0, \tag{12a}$$

and

$$\theta=\theta_{\mathrm{R}}\quad\text{at }\eta=1. \tag{12b}$$

The dimensionless forms of the coupled ordinary differential equations (6a)–(6d) are

$$\frac{\mathrm{d}\tilde{\psi}_0}{\mathrm{d}\eta}=-3\tau_0\tilde{\psi}_1+\frac{14}{3}\tau_0\tilde{\psi}_3, \tag{13a}$$

$$\frac{\mathrm{d}\tilde{\psi}_1}{\mathrm{d}\eta}=4\tau_0(1-\omega)\theta^4-(1-\omega)\tau_0\tilde{\psi}_0, \tag{13b}$$

$$\frac{\mathrm{d}\tilde{\psi}_2}{\mathrm{d}\eta}=\frac{-7}{3}\tau_0\tilde{\psi}_3, \tag{13c}$$

$$\frac{\mathrm{d}\tilde{\psi}_3}{\mathrm{d}\eta}=\frac{-8}{3}\tau_0(1-\omega)\theta^4+\frac{2}{3}\tau_0(1-\omega)\tilde{\psi}_0-\frac{5}{3}\tau_0\tilde{\psi}_2, \tag{13d}$$

and the corresponding dimensionless radiative boundary conditions (7a)–(7d) are:

$$(1-\rho_{\mathrm{L}})\tilde{\psi}_0(0)+2(1+\rho_{\mathrm{L}})\tilde{\psi}_1(0)+\frac{5}{4}(1-\rho_{\mathrm{L}})\tilde{\psi}_2(0)-4\varepsilon_{\mathrm{L}}\theta_{\mathrm{L}}^4=0, \tag{14a}$$

$$(1-\rho_{\mathrm{L}})\tilde{\psi}_0(0)+\frac{12}{5}(1+\rho_{\mathrm{L}})\tilde{\psi}_1(0)+\frac{5}{2}(1-\rho_{\mathrm{L}})\tilde{\psi}_2(0)+\frac{8}{5}(1+\rho_{\mathrm{L}})\tilde{\psi}_3(0)-4\varepsilon_{\mathrm{L}}\theta_{\mathrm{L}}^4=0, \tag{14b}$$

$$(1-\rho_{\mathrm{R}})\tilde{\psi}_0(\tau_0)-2(1+\rho_{\mathrm{R}})\tilde{\psi}_1(\tau_0)+\frac{5}{4}(1-\rho_{\mathrm{R}})\tilde{\psi}_2(\tau_0)-4\varepsilon_{\mathrm{R}}\theta_{\mathrm{R}}^4=0, \tag{14c}$$

$$(1-\rho_R)\tilde{\psi}_0(\tau_0)+\frac{12}{5}(1+\rho_R)\tilde{\psi}_1(\tau_0)+\frac{5}{2}(1-\rho_R)\tilde{\psi}_2(\tau_0)$$
$$-\frac{8}{5}(1+\rho_R)\tilde{\psi}_3(\tau_0)-4\varepsilon_R\theta_R^4=0. \tag{14d}$$

Here $\tau_0=\beta L$ is the optical thickness, and $N=\frac{\rho_d c_p T_0 C}{\sigma T_0^4}$ is so called conduction-to-radiation parameter.

For the Fourier law of conduction, the dimensionless energy and flux equations (9) and (10), when combined, reduce to

$$\frac{\partial\theta(\eta,\xi)}{\partial\xi}-\frac{1}{M}\frac{\partial^2\theta(\eta,\xi)}{\partial\eta^2}+\frac{1}{N}\frac{\partial Q^r(\eta,\xi)}{\partial\eta}=0, \tag{15}$$

where the initial, boundary conditions, and radiation heat flux equations remain the same as those given by Eqs. (11)–(14), respectively.

3. Numerical method

The non-Fourier problem considered above involves a discontinuity at the wave front. MacCormack's predictor–corrector scheme has been shown to handle moving discontinuities quite well [20–24,28,29] and is thus chosen for the present study. The scheme can be characterized as an explicit second-order accurate predictor–corrector sequence for the integration of partial differential equations and coupled with the P_3 approximation method to solve the combined non-Fourier heat conduction problem with radiation in the participating medium. In order to apply MacCormack's scheme, Eqs. (9) and (10) are written in vector form as

$$\frac{\partial E}{\partial\xi}+\frac{\partial F}{\partial\eta}+H=0, \tag{16a}$$

where

$$E=\begin{bmatrix}\theta\\ Q^c\end{bmatrix},\qquad F=\begin{bmatrix}(Q^c+Q^r)/N\\ N\theta\end{bmatrix},\qquad H=\begin{bmatrix}0\\ MQ^c\end{bmatrix}. \tag{16b}$$

Then, Eq. (16a) is expanded by the finite differences and explicit method, we have Predictor

$$\hat{E}_i^{n+1}=E_i^n-\frac{\Delta\xi}{\Delta\eta}(F_{i+1}^n-F_i^n)-\Delta\xi H_i^n, \tag{17a}$$

Corrector

$$\hat{E}_i^{n+1}=\frac{1}{2}\left[E_i^n+\hat{E}_i^n-\frac{\Delta\xi}{\Delta\eta}(\hat{F}_i^{n+1}-\hat{F}_{i-1}^{n+1})-\Delta\xi\hat{H}_i^{n+1}\right]. \tag{17b}$$

Here, the subscript i denotes the grid points in the space domain, superscripts n and $n+1$ denote the time levels, the tilde refers to the predicted value at the time level $n+1$, and $\Delta\eta$ and $\Delta\xi$ are the space and time steps, respectively.

Eqs. (16), along with the initial, boundary conditions, and radiation heat flux equations, Eqs. (11)–(14), constitute the complete non-Fourier mathematical formulation of heat transfer

problem. The BVPFD subroutine of the commercially available IMSL software library can be used to solve the system of coupled ordinary differential equations with boundary conditions at two points, using a variable order, variable step size, finite-difference method with deferred corrections. The subroutine has been employed to solve the coupled differential equations of intensity of radiation, and then one of the solutions, $\tilde{\psi}_1(\eta)$, is the net radiative heat flux, $Q^{\mathrm{r}}(\eta)$, that we need in the temperature-computing processes. First, the temperature is calculated by inserting the initial conditions into Eqs. (17a) and (17b). Then substitute the new temperature distributions into Eqs. (13a)–(13d), and obtain the radiative heat flux at each time step. Subsequently, they are then substituted into Eqs. (17a) and (17b) to obtain new temperature distributions and conduction heat fluxes at the next time step. The above procedure is repeated until the system reaches the steady-state convergence criterion

$$\frac{\max\left|\theta_i^{n+1}-\theta_i^n\right|}{\left|\theta_i^{n+1}\right|}\leqslant 10^{-5}. \tag{18}$$

For the Fourier heat conduction with body radiation, the Crank–Nicolson method is used to integrate the parabolic heat conduction equation, Eq. (15), while the radiative heat transfer is still solved using the P_3 approximation method to ensure accurate solutions. The BVPFD subroutine is also used to solve the system of coupled ordinary differential equations.

4. Results and discussion

Following the work of Glass et al. [24], the dimensionless variable $M=LC/\alpha$ is set to be 2, and the refractive index of the medium is taken as unity. For all cases considered, we have taken $\varepsilon_{\mathrm{L}}=\varepsilon_{\mathrm{R}}=1.0$, $\rho_{\mathrm{L}}=\rho_{\mathrm{R}}=0.0$ (for black surfaces), maintaining the left boundary at $\theta_{\mathrm{L}}=1.0$ and the other side at $\theta_{\mathrm{R}}=\theta_0=0.0$.

Grid refinement and time step sensitivity studies were performed for the physical model to ensure that the essential physics are independent of grid size and time interval. Fig. 2 presents the temperature distributions with three different grid sizes of uniform 201, 501, and 801, for conduction-to-radiation parameter $N=10.0$, optical thickness $\tau_0=1.0$ and single scattering albedo $\omega=0.0$ at three different times, respectively. The hyperbolic wave nature of non-Fourier heat conduction is clearly shown by the sharp wave front displayed. The results from 201 grids exhibit a high degree of dispersion, but without oscillations near the wave front. In contrast, a minor degree of dispersion, but with oscillations near the discontinuities are present in the results from 801 grids. Yang [29] suggested that the oscillations near discontinuities could not be avoided when the finite-difference scheme was used to solve the hyperbolic heat conduction equation. Glass et al. [28] suggested a way to decrease the oscillations: increase the mesh size, i.e., decrease the computation grids. In all the cases studied, 501 grids were found to exhibit small degree of dispersion and no oscillations near the wave front. Uniform 501 grids system with Courant number of $v=\Delta\eta/\Delta\xi=0.98$ were used to generate the presented results (with small value of v, oscillations near discontinuities are enlarged [24]).

The effects of single scattering albedo ω, conduction-to-radiation parameter N, and optical thickness τ_0 of the medium on the transient and steady-state temperature distribution are investigated in detail. For all the figures, the hyperbolic solutions of non-Fourier heat conduction are

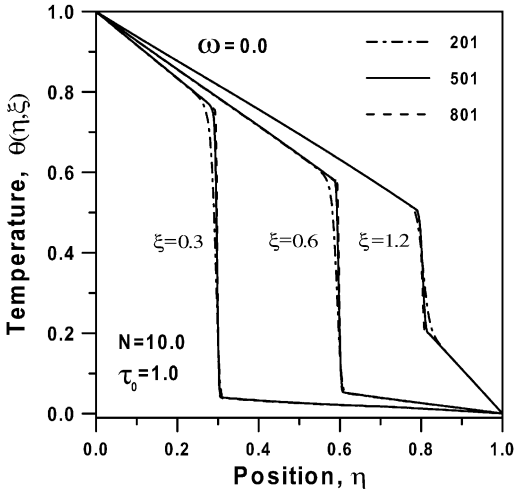

Fig. 2. Temperature distributions with three different grid sizes for $N = 10.0$, $\tau_0 = 1.0$ and $\omega = 0.0$.

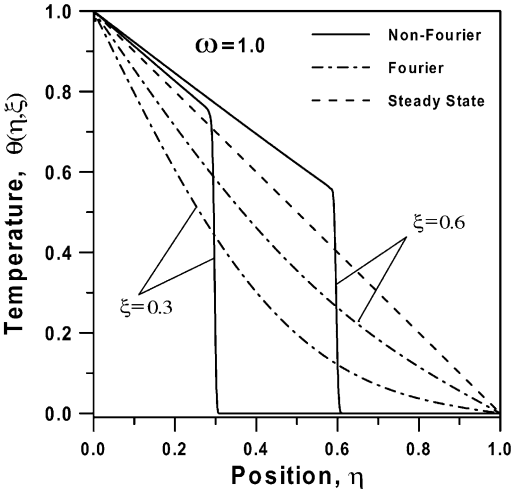

Fig. 3. Temperature distributions for a purely scattering medium of single scattering albedo $\omega = 1.0$.

shown by solid lines, while the Fourier and steady-state (same for non-Fourier and Fourier heat conduction) solutions are shown by broken lines.

Fig. 3 shows the transient and steady temperature distributions for a purely scattering medium (single scattering albedo $\omega = 1.0$). A purely scattering medium cannot absorb radiative heat fluxes. Therefore, the temperature profiles are the same as those for purely conductive case in transient history and also in the steady state. This phenomenon is similar to what happened in another combined parabolic heat conduction and radiation case [1]. Without considering the internal radiation, the hyperbolic equation of non-Fourier conduction, different from the diffusion equation of Fourier conduction, predicts that a thermal wave disturbance tends to propagate in a given direction at a given propagation speed until its course is impeded by a wall or barrier. Since the dimensionless wave speed is unity, the wave front located at position $\eta = 0.3$ (0.6) at time $\xi = 0.3$ (0.6), and an undisturbed region is found ahead of its front. Obviously, the thermal waves propagate toward the right boundary by time $\xi = 0.6$, when the time passes, the reflection waves from the right boundary propagating toward the left boundary will appear until a smooth temperature distribution that steady state has been reached. The non-Fourier effect on heat conduction is a short-time behavior. The steady-state temperature distribution for non-Fourier conduction is the same as that for Fourier conduction.

Figs. 4(a) and (b) illustrate the effects of the single scattering albedo ω on the transient and steady-state temperature distributions for $N = 1.0$ and $\tau_0 = 1.0$ with $\omega = 0.0$ and 0.5, respectively. Note that the temperature profiles for purely scattering case $\omega = 1.0$ are the same as for pure conduction just discussed above in Fig. 3, while, the temperature profiles for $\omega = 0.0$ are the same as those for a pure absorbing, emitting medium. When radiative effect is taken into accounted, the radiation is found to enhance the heat transport in the medium. Because of low scattering (a smaller value of ω), a larger amount of radiation energy is absorbed in

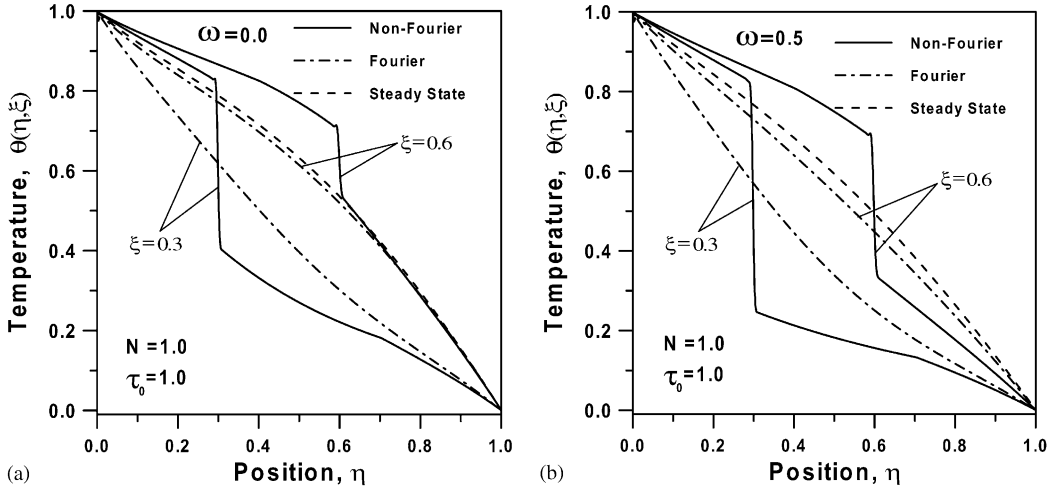

Fig. 4. Effects of single scattering albedo ω on temperature distribution for $N = 1.0$, $\tau_0 = 1.0$ with (a) $\omega = 0.0$ and (b) $\omega = 0.5$.

the medium, in both Fourier and non-Fourier cases, decreasing the value of ω increases the temperature profiles. For non-Fourier heat conduction, due to a smaller scattering albedo, the medium is heated by the larger amount of radiation, resulting in a smaller temperature front propagating from the right surface. The sharp wave front of hyperbolic nature from non-Fourier effect has been smoothened by the strong radiative effect by decreasing the value of scattering albedo ω. The wave nature of combined non-Fourier heat conduction and radiation is more obvious in a more highly scattering medium. In other words, the effects of radiation on thermal wave propagation are more pronounced in a non-scattering medium. As time passes, the effect of scattering on temperature profiles becomes less evident since heat conduction is dominated by diffusion. This resembles the results in Fig. 3 mentioned above.

Figs. 5(a) and (b), along with Fig. 4(b), display the effects of conduction-to-radiation parameter N on the transient and steady-state temperature distributions for $\omega = 0.5$ and $\tau_0 = 1.0$ with $N = 0.1$, 10.0 and 1.0, respectively. The conduction-to-radiation parameter is taken as $N = 0.1$, 1.0 and 10.0, which can represent the radiation effects from the strong to the weak radiation. As expected, both Fourier and non-Fourier cases, decreasing the value of N increases the temperature profiles. The non-Fourier effects become insignificant as either time increases or conduction-to-radiation parameter N decreases.

Figs. 6(a) and (b), along with Fig. 4(b), demonstrate the effects of optical thickness τ_0 on the transient and steady-state temperature distributions for $\omega = 0.5$ and $N = 1.0$ with $\tau_0 = 0.1$, 10.0 and 1.0, respectively. The different values of optical thickness studied include $\tau_0 = 0.1$, 1.0 and 10.0, which characterize the cases from optically thin to optically thick. An optically thin medium absorbs a relatively smaller amount of radiation than an optically thick one. Thus, increasing the value of τ_0 increases the temperature profiles for both Fourier and non-Fourier cases, and the non-Fourier effects become insignificant as either time increases or the optical thickness τ_0 increases. Due to a larger optical thickness, the medium is heated by the larger amount of radiation, resulting in a smaller temperature front propagating from the right surface.

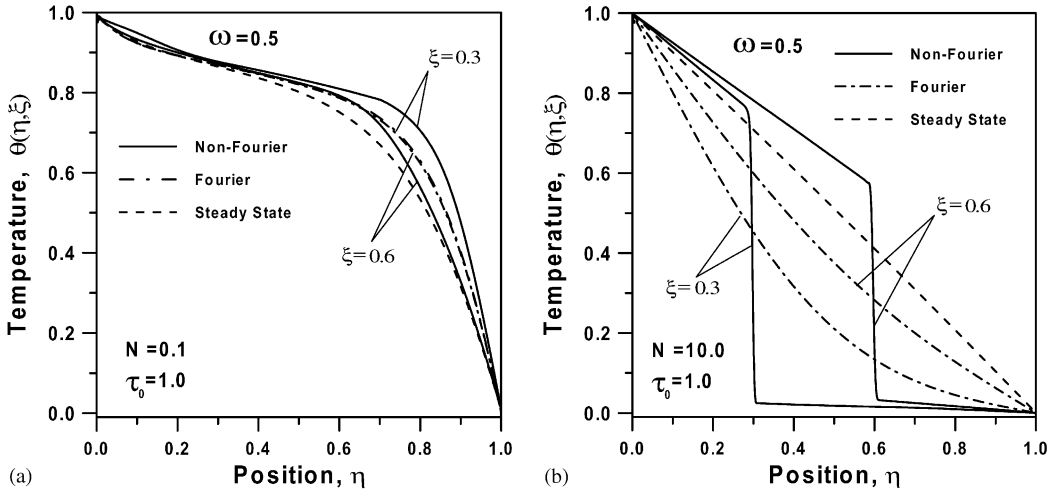

Fig. 5. Effects of conduction-to-radiation parameter N on temperature distributions for $\omega = 0.5$, $\tau_0 = 1.0$ with (a) $N = 0.1$ and (b) $N = 10.0$.

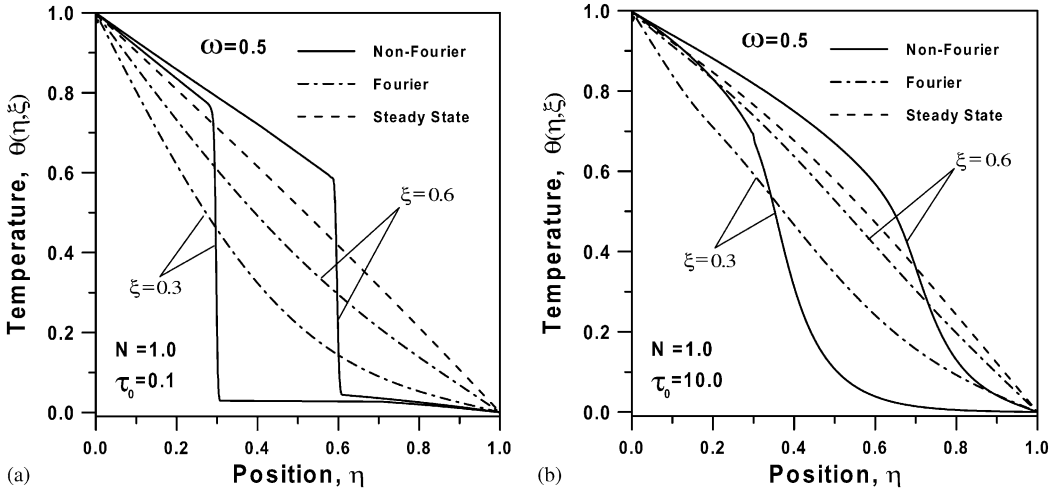

Fig. 6. Effect of optical thickness τ_0 on temperature distributions for $\omega = 0.5$, $N = 1.0$ with (a) $\tau_0 = 0.1$ and (b) $\tau_0 = 10.0$.

The sharp wave front of hyperbolic nature from non-Fourier effect has been smoothened by increasing the value of optical thickness τ_0. The wave nature is more obvious for optically thin medium. In other words, the effects of radiation on thermal wave propagation are more pronounced in an optically thin medium. The radiative heat flux vanishing in both limits at zero and infinite optical thickness implies that the highest radiative heat loss occurs somewhere in the intermediate optical thickness. This lead temperature profiles in steady state decreases with increasing optical thickness until one critical value of τ_0 is reached, and then diminishes beyond that point.

5. Conclusion

Transient and steady behavior of non-Fourier-effect in heat conduction with radiation in a gray, absorbing, emitting, and isotropically scattering one-dimensional medium has been presented. Boundary surfaces were considered to be black, diffusely emitting, diffusely reflecting and isothermal. The P_3 approximation method was employed to treat the equation of radiative heat transfer, while MacCormack's explicit predictor–corrector scheme was used to solve the hyperbolic heat conduction equation.

The effects of radiation on the thermal wave propagation in the medium were examined using three radiation parameters: single scattering albedo, conduction-to-radiation parameter, and optical thickness. The radiation effect is more pronounced at small values of single albedo, small values of conduction-to-radiation parameter, and large values of optically thickness. Analysis results demonstrate that the hyperbolic sharp wave front of non-Fourier conduction becomes smoother when radiative heat transfer is taken into account. The wave nature is more obvious in a highly scattering, a larger conduction-to-radiation parameter, and an optically thin medium. In a purely scattering medium, the thermal behavior is reduced to that of pure conduction. These three parameters more significantly affect transient temperature distribution than steady-state temperature distribution. The results from non-Fourier-effect equation are also compared to those obtained from the Fourier equation. Non-Fourier effect becomes insignificant as either time increases or the effect of radiation increases.

Acknowledgements

This research was supported by the National Science Council of Taiwan, ROC through Grant NSC 89-2218-E-009-039.

References

[1] Özisik MN. Radiative transfer and interactions with conduction and convection. New York: Wiley-Interscience, 1973.
[2] Viskanta R. Radiation transfer: interaction with conduction and convection and approximate methods in radiation. In Heat Transfer 1982, Proceedings of the 7th International Heat Transfer Conference, Munich 1982, vol. 1. Washington, DC: Hemisphere, 1982. p. 103–21.
[3] Siegel R. Transient thermal effects of radiant energy in translucent materials. ASME J Heat Transfer 1998;120:4–23.
[4] Yuen WW, Wong LW. Heat transfer by conduction and radiation in a one-dimensional absorbing, emitting and anisotropically-scattering medium. ASME J Heat Transfer 1980;102:303–7.
[5] Fernandes R, Francis J. Combined conductive and radiative heat transfer in an absorbing, emitting, and scattering cylindrical medium. ASME J Heat Transfer 1982;104:594–601.
[6] Tsai JR, Özisik MN. Transient, combined conduction and radiation in an absorbing, emitting, and isotropically scattering solid sphere. JQSRT 1987;38:243–51.
[7] Ratzel AC, Howell R. Heat transfer by conduction and radiation in one-dimensional planar media using the differential approximation. ASME J Heat Transfer 1982;104:388–91.
[8] Chu HS, Tseng CJ. Thermal performance of ultra-fine powder insulations at high temperatures. J Thermal Insulation 1989;12:298–312.

[9] Chu HS, Weng LC. Transient combined conduction and radiation in anisotropically scattering spherical media. J Thermophys Heat Transfer 1992;6:553–6.
[10] Tseng CJ, Chu HS. Transient combined conduction and radiation in an absorbing, emitting, and anisotropically-scattering medium with variable thermal conductivity. Int J Heat Mass Transfer 1992;35: 1844–7.
[11] Sakami M, Charette A, Le Dez V. Application of the discrete ordinates method to combined conductive and radiative heat transfer in a two-dimensional complex geometry. JQSRT 1996;56:517–33.
[12] Yao CC, Chung BTF. Transient heat transfer in a scattering-radiating-conducting layer. J Thermophys Heat Transfer 1999;13:18–24.
[13] Wu JW, Chu HS. Combined conduction and radiation heat transfer in plane-parallel packed beds with variable porosity. JQSRT 1999;61:443–52.
[14] Lazard M, André S, Maillet D. Transient coupled radiative-conductive heat transfer in a gray planar medium with anisotropic scattering. JQSRT 2001;69:23–33.
[15] Özisik MN, Tzou DY. On the wave theory in heat conduction. ASME J Heat Transfer 1994;116:526–35.
[16] Glass DE, Tamma KK. Non-Fourier dynamic thermoelasticity with temperature-dependent thermal properties. J Thermophys Heat Transfer 1994;8:145–51.
[17] Tzou DY. Macro- to microscale heat transfer: the lagging behavior. Washington, DC: Taylor & Francis, 1996.
[18] Tamma KK, Zhou X. Macroscale and microscale thermal transport and thermo-mechanical interactions: some noteworthy perspectives. J Thermal Stresses 1998;21:405–49.
[19] Tan ZM, Yang WJ. Propagation of thermal waves in transient heat conduction in a thin film. J Franklin Institute 1999;336B:185–97.
[20] Wu JP, Chu HS. Propagation and reflection of thermal waves in a rectangular plate. Numer Heat Transfer Part A 1999;36:51–74.
[21] Lor WB, Chu HS. Hyperbolic heat conduction in thin-film high T_c superconductors with interface thermal resistance. Cryogenics 1999;39:739–50.
[22] Lor WB, Chu HS. Propagation of thermal waves in a composite medium with interface thermal boundary resistance. Numer Heat Transfer Part A 1999;36:681–97.
[23] Lor WB, Chu HS. Effect of interface thermal resistance on heat transfer in a composite medium using the thermal wave model. Int J Heat Mass Transfer 2000;653–63.
[24] Glass DE, Özisik MN, McRae DS. Hyperbolic heat conduction with radiation in an absorbing and emitting medium. Numer Heat Transfer 1987;12:321–33.
[25] Joseph DD, Preziosi L. Heat waves. Rev Mod Phys 1989;61:41–73.
[26] Cattaneo C. A form of heat conduction equation which eliminates the paradox of instantaneous propagation. Comput Rendus 1958;247:431–3.
[27] Vernotee P. Les paradoxes de la theorie continue de l equation del la Chaleur. Comput Rendus 1958;246: 3154–5.
[28] Glass DE, Özisik MN, McRae DS, Vick B. On the numerical solution of hyperbolic heat conduction. Numer Heat Transfer 1985;8:497–504.
[29] Yang HQ. Characteristics-based, high order accurate and nonoscillatory numerical method for hyperbolic heat conduction. Numer Heat Transfer Part B 1990;18:221–41.